# Dalton Transactions

Accepted Manuscript






ROYAL SOCIETY OF CHEMISTRY

www.rsc.org/dalton

# Influence of the binding of reduced NAMI-A to human serum albumin on the pharmacokinetics and biological activity

V. Novohradský[1,2], A. Bergamo[3], M. Cocchietto[3], J. Zajac[1,2], V. Brabec[1], G. Mestroni[3], G. Sava[3,4]

[1]Institute of Biophysics, Academy of Sciences of the Czech Republic, v.v.i., Kralovopolska 135, CZ-61265 Brno, Czech Republic. Fax: +420 541240499; Tel: +420 541517148

[2]Department of Biophysics, Faculty of Science, Palacky University, 17. Listopadu 12, CZ-77146 Olomouc, Czech Republic

[3]Callerio Foundation Onlus, via A. Fleming 22, 34127-Trieste, Italy

[4]Department of Life Sciences, University of Trieste, via A. Fleming 22, 34127-Trieste, Italy.

ABSTRACT

NAMI-A is a ruthenium-based drug endowed with the unique property of targeting selectively solid tumour metastases. Although two clinical studies had already been completed, very poor information exists on the behavior of NAMI-A once injected into the bloodstream. PK data in humans inform us of a rather low free drug concentration, of a relatively high half-life time of elimination and of a linear relationship between the administered dose and the corresponding AUC up to toxic doses. With the present study we examined the chemical kinetics of albumin binding in the presence or not of reducing agents and we evaluated how these chemical aspects might influence the in vivo PK and the in vitro ability of NAMI-A to inhibit cell migration, a bona fide rapid and easy way to suggest anti-metastatic properties.

Overall, the experimental data support the binding of NAMI-A to serum albumin, a reaction facilitated when the drug is in its reduced form and, in agreement with already reported data, the maintenance of the biological activity of the adduct formed with albumin. The formation of the adduct is favored by low ratios NAMI-A:HSA and by the reduction of the drug with ascorbic acid.

The different in vivo PK and the faster binding to albumin of the reduced NAMI-A seem to exclude that the drug is rapidly reduced immediately upon injection, even at low doses. Most probably, cell and protein binding prevail over the reduction of the drug. This observation supports the thesis that the reduction of the drug before injection must be considered relevant for the pharmacological activity of NAMI-A against tumour metastases.

INTRODUCTION

The development of metal based compounds as drugs for the treatment of the cancer disease, initially focused almost only on platinum, is today extended to other transition metals among which ruthenium appears to be one of the most attractive (Page et al., 2009; Antonarakis and Emadi, 2010; Komeda and Casini, 2012). There are objective and opportunistic reasons to stress the role of ruthenium for metal-based anticancer drugs. The main objective reason is that related to the generally more tolerated toxicity of the ruthenium compounds than the classical platinum complexes, when tested in living beings (Bergamo et al., 1999; Hartinger et al., 2008; Meng et al., 2009; Vadori et al., 2013). The opportunistic reason is that among the many metal compounds synthesized and studied in more than 50 years, after the discovery of cisplatin, only two ruthenium complexes, namely imidazolium *trans*-imidazoledimethylsulphoxide-tetrachlororuthenate (NAMI-A) and sodium *trans*-*bis*-indazoletrachlororuthenate (KP1339) have moved to clinical studies in humans (Rademaker-Lakhai et al., 2004; Hartinger et al., 2006). NAMI-A is attractive because of the ability to target solid tumor metastases rather than to exert a non-selective tumor toxicity (Sava et al., 1998; Sava et al., 1999; Bergamo et al., 1999; Sava et al., 2003). In fact, tumor metastases represent the main target of cancer chemotherapy and their eradication is the only way to cure a cancer disease (Deng et al., 2014; McLoughlin et al., 2006; McCusker et al., 2014; Shiiba et al., 2014). NAMI-A, although with a still only-presumed target and mechanism of action (Sava et al., 2004; Frausin et al., 2005; Gava et al., 2006; Bergamo et al., 2012), represents the metal-based compound endowed with innovative properties, matching an unmet need of oncological treatments. If there is very little doubt about the metastasis selectivity (Sava et al., 1998; Sava et al., 1999; Sava et al., 2003), very poor information exists on the behavior of NAMI-A once injected into the bloodstream. PK data in humans inform us of a rather low free drug concentration, of a relatively high half-life time of elimination and of a linear relationship between the administered dose and the corresponding AUC up to toxic doses (Rademaker-Lakhai et al., 2004). However at least two questions are still open: a) what is the preferred oxidation state of the metal center with which NAMI-A binds to plasma proteins? and b) is the albumin-

adduct endowed with the same biological activities of free NAMI-A? Both these questions relate to the chemical behavior of NAMI-A in biological solutions (Bouma et al., 2002; Alessio et al., 2004; Bacac et al., 2004), and to the role of the biological reducing agents such as ascorbic acid or glutathione that are present in circulation (Brindell et al., 2007). Since the species responsible for the effects on tumor metastases is still unknown, any further information on reduction, that was shown responsible for the speciation of the compound in solution (Sava et al., 2002; Webb and Walsby, 2011), and albumin binding, recently demonstrated to markedly influence the maintenance of the original ligands in the coordination sphere (Brindell et al., 2008; Ascone et al., 2008; Liu et al., 2010; Webb and Walsby, 2011), would help to understand the nature of the active species of NAMI-A and most hopefully to suggest what kind of structure modification is required to increase the ratio between activity and toxicity. We therefore thought it worth to study the chemical kinetics of albumin binding in the presence or not of reducing agents, as occurs in the bloodstream, and to evaluate how these chemical aspects would influence the in vivo PK and the in vitro ability of NAMI-A to inhibit cell migration, a bona fide rapid and easy way to suggest anti-metastatic properties.

## MATERIALS AND METHODS

**Chemicals.** Imidazolium *trans*-imidazole(dimethylsulfoxide)tetrachloro-ruthenate ImH [*trans*-$RuCl_4$(DMSO)Im] (NAMI-A) was synthesized by Serichim (Torviscosa, Italy) according to already described procedures (Mestroni et al., 1998). All reagents were purchased from Sigma-Aldrich (St. Louis, MO, USA), unless otherwise indicated.

**Preparation of Stock Solutions.** NAMI-A, HSA and ascorbic acid were dissolved immediately before use in DPBS (Dulbecco's phosphate buffered saline), pH=7.4, respectively to the final concentration of 10, 0.5 and 20 mM.

**Spectrophotometric Experiments.** Spectrophotometric data were obtained using Jasco V-550 at the range of wavelengths from 700 nm to 300 nm, with a scanning speed set at 200 nm/min, band with 1.0 nm and data pitch 1.0 nm. Spectra were measured with the interval of 5 min. If not otherwise stated spectra were measured at 25 °C with a final volume of 3 ml. Temperature of the reaction solution was monitored and controlled using a Peltier control accessory. Spectra were processed with GraphPad Prism 4 software.

**Interaction with Human Serum Albumin.** 100 μM NAMI-A was exposed to HSA at the ratios 4:1, 2:1, 1:1 and 0.25:1 in DPBS under constant temperature of 25 °C, pH 7.4. NAMI-A was added to solutions of HSA and the reaction was monitored up to 145 min.

**Interaction of NAMI-A with HSA in solution upon reduction by ascorbic acid.** NAMI-A at the concentration of 400 μM was reduced by 100, 50 and 2.5 μM of ascorbic acid in the presence of 100 μM of HSA. NAMI-A and ascorbic acid were added together to the solution of HSA. The reaction was carried out at 25 °C, pH 7.4 with a final volume of 3 ml.

**In vitro studies**.

*Tumour cell line*. The MDA-MB-231 human highly invasive breast cancer cell line was kindly supplied by Dr. P. Spessotto (Cro, Aviano, Italy) and maintained in Dulbecco's modified Eagle's medium supplemented with 10% FBS (Foetal Bovine Serum, Gibco, Invitrogen™, Paisley, Scotland, UK), 2 mM L-glutamine, 1% non-essential amino acids and 100 IU/ml penicillin and 100 μg/ml streptomycin (all the reagents of this paragraph were from EuroClone®, Devon, UK)).

The cell line was kept in an incubator with 5% $CO_2$ and 100% relative humidity at 37°C. Cells from a confluent monolayer were removed from flasks by a trypsin-EDTA solution. Cell viability was determined by the trypan blue dye exclusion test. For experimental purposes cells were sown in multi-well cell culture clusters.

*Re-adhesion assay*. To study the effect of the treatments on the cell ability to re-adhere to a growth substrate cells were sown in complete medium in cell culture flasks and let grow for 2 days at 37 °C 5% $CO_2$, then complete medium was replaced with serum-starved medium containing 0.1% w/v BSA for 24 h before treatment with NAMI-A (1÷100 μM), ascorbic acid (0.5÷100 μM), HSA (25÷400 μM) or with their combination, at the ratios reported in

the legend of the relative figures, in DPBS for 1 h at 37 °C 5% $CO_2$. At the end of the treatment cells were removed from flasks by a trypsin-EDTA solution, collected by centrifugation, re-suspended in serum-starved medium supplemented with 0.1% w/v BSA and kept for 30 min at room temperature to allow surface receptor reconstitution. The cells were then seeded at a density of $1x10^4$ cells in 0.1 ml/well on 96-well plastic plates. Cells were left to adhere for 30 min at 37 °C 5% $CO_2$, then the medium containing the non-adhered cells was removed and wells were gently washed with $Ca^{+2}Mg^{+2}$ free-DPBS. Cells that in 30 min have adhered to the substrate were detected by the sulforhodamine B (SRB) test.

*Sulforhodamine B assay*. Adherent cells were detected with the SRB test described by Skehan et al. (Skehan et al., 1990). Briefly, adherent cells were fixed with 10% v/v cold trichloroacetic acid (TCA) at 4 °C for 1 h. After fixation TCA was discarded and wells washed five times with distilled water and air-dried. SRB solution (0.4% w/v in 1% acetic acid) was added to the wells for 30 min at room temperature (RT). Unbound SRB was removed by washing three times with 1% acetic acid. Plates were air-dried, then bound stain was dissolved with un-buffered 10 mM Tris base (tris-hydroxymethyl-aminomethane) at pH 10.5 and the absorbance units were read at 570 nm with a spectrophotometer (SpectraCount, Packard, Meriden, CT, USA).

**In vivo studies**.

*Animals*. Experiments on animals were carried out on 10 weeks old ICR (CD-1) male mice, according to the guidelines in force in Italy (DDL 116 of 21/2/1992) and in compliance to the Guide for Care and Use of Laboratory Animals, Department of Health and Human Services Publication No. (NIH) 86-23, Bethesda, MD, National Institutes of Health, 1985. The average animal weight was 39.0 ± 3.5 g (range 33.0 - 48.4 g).

*In Vivo Treatments*. Compounds were administered i.v. through the lateral tail vein. NAMI-A was applied at the dose 50mg/kg body weight and dissolved in sterile DPBS immediately before use in an appropriate volume in order to inject 0.05 ml/10 g body weight. For the calculation of the appropriate dose for each animal the mice were weighted one day (24 h) before the treatment. NAMI-A and reduced form of NAMI-A were incubated in DPBS

and/or in DPBS with ascorbic acid for 5 min at 37 °C before the administration. The molar ratio of NAMI-A to ascorbic acid was 1:1. Intravenous application to the tale vein was done after the vasodilatation with hot water. Animals were anesthetized with i.p. injection of Zoletil (tiletamine/zolazepam) 15 mg/kg and Xilor (xylazine) 5 mg/kg. Samples were collected at 0, 10, 20, 40 minutes, 1, 2, 4 and 24 h from three mice per group in each time point.

*Samples collection*. The blood withdrawal was performed by heart puncture on anesthetized animals. Plasma was separated with centrifugation at 2000 g for 3 min at room temperature using heparin (50 U/ml of blood) as anticoagulation agent. Urine was collected, on animals killed by cervical dislocation and opened by surgery, by bladder puncture. Liquid samples were immediately frozen in the liquid nitrogen and stored at -80°C until analysis. Fragments of lungs, liver and kidney were carefully removed, weighted, and immediately frozen in liquid nitrogen. Samples were stored at -80°C until further processing.

*FAAS analysis - samples processing*. Liquid samples were digested with tetramethylammoniumhydroxide (TMAH) at 25% in Milli-Q water, with a 1:5 sample:TMAH ratio at room temperature, in closed Nalgene cryovials (Nalge Company, Rochester, NY, USA) and under continuous agitation for at least 24 h, according to a procedure adapted from that described by Tamura et al. (1992). The solid organ samples were firstly heated in an oven at 105 °C until completely dried. The organ fragments were then completely dissolved in closed Nalgene cryovials by the addition of 0.5 ml of 25% TMAH in water, at room temperature and under continuous agitation, for at least 24 h. When the digestion occurred, the final volume was adjusted to 1 ml with Milli-Q water.

*FAAS measurements*. Ruthenium concentration in plasma samples was measured using a graphite furnace atomic absorption spectrometer, model SpectrAA-220Z, supplied with GTA 110Z, an autosampler PSD 100 and a specific ruthenium hollow cathode emission lamp (all Agilent, Mulgrave, VIC, Australia). Ruthenium concentration in urine and organs was measured using an analogue instrumentation composed by: an AA240Z Zeeman atomic absorption spectrometer equipped with a GTA 120 graphite tube atomizer, an autosampler PSD 110 and a specific ruthenium hollow cathode emission lamp (all Agilent,

Mulgrave, VIC, Australia). The lower and higher limits of quantification were set at the levels corresponding to the lower and higher standard concentration i.e. 20 and 100 ng of ruthenium per mL, respectively. The limit of detection of 10 ng of ruthenium per mL was estimated according to the EURACHEM guide (http://www.eurachem.org/). The quantification of ruthenium was carried out in 10 µl samples at 349.9 nm with an atomizing temperature of 2,600°C. Argon was used as purge gas at a flow rate of 3 l/min. Before each analysis session, a five point calibration curve was traced using ruthenium standard, 992 µg/ml.

**Statistical analysis.** Results obtained were processed using GraphPad InStat software and presented as mean ± standard deviation. The group means were compared using a Two-Way Analysis of Variance (ANOVA) and Tukey-Kramer Multiple Comparisons Test and considered significant when $p < 0.05$.

## RESULTS AND DISCUSSION

The results of the present investigation will be presented and discussed in the light of the tests done in humans in the phase I trial for dose and toxicity finding (Rademaker-Lakhai et al., 2004) and for the pharmacological effects in combination with gemcitabine in a phase I/II study in patients with NSCLC (Leijen, 2013).

A number of papers have discussed the role of albumin in the activity of NAMI-A and its influence on the chemical behavior in solution (Messori et al., 2000; Bergamo et al., 2003; Ascone et al., 2008; Liu et al., 2010; Webb and Walsby, 2011; Levina et al., 2013), as well as the role of adducts formed by compounds with different metal centers with other macromolecules (i.e. Pt with RNA, Hostetter et al., 2012). When NAMI-A is injected intravenously in patients by slow infusions, at doses of 300-450 mg/m$^2$ [corresponding to about 530-780 mg NAMI-A/patient (about 1.1-1.7x10$^{-3}$ total moles/patient)] (see the phase I/II in combination with gemcitabine, Leijen, 2013), the expected NAMI-A:HSA ratio at the site of contact, e.g. in the vein in which the catheter for injection is positioned, should

be about 3.5-5.2 (estimated HSA in blood= $0.65x10^{-3}$ M). In fact, with a rate of infusion of 2.8 ml/min (500 ml in 3 h), NAMI-A gets into the vein at a molar concentration of 2.3-$3.4x10^{-3}$ M, respectively at the doses of 300 and 450 mg/m$^2$. However, the subsequent dilution of NAMI-A in the blood compartment (estimating a volume of serum of about 3 l), might reduce this ratio to about 0.58-0.87.

*Effects of human serum albumin.*

Data of Figure 1 show the rate of transformation of NAMI-A in DPBS pH=7.4 at 25°C, evidencing the loss of the peaks of intact NAMI-A at 390 nm and that of the hydroxo derivative at 345 nm, with formation of further degradation species at wavelengths lower than those explored here. The study of the interactions between NAMI-A and human serum albumin reported in Figure 2 suggests that with ratios NAMI-A:HSA from 4 to 0.25, the rate of the above reactions is progressively increased; at the ratio NAMI-A:HSA=1 they are markedly accelerated [Figure 2, lower panel, left] and at the ratio=0.25 (Figure 2, lower panel, right) the transformation of NAMI-A and the formation of the adduct with albumin goes to completion in a very short time.

The examination of the pharmacokinetic parameters of NAMI-A in the patients confirmed the high NAMI-A binding to the plasma proteins with almost 98-99% of the drug found in the whole plasma and with only 1-2% or less in the protein free plasma (ultra-filterable plasma) at any of the dosages tested from 2.4 to 600 mg/m$^2$ (Rademaker-Lakhai et al., 2004; Leijen, 2013). Interestingly, the peak concentration of drug in the plasma, at the end of the infusion, accounts for about 30-40% of the administered dose, independently of the dose-level used. Similarly, also the decay of blood concentration of the drug, due to kidney elimination, is linear with the administered dose and accounts for the loss of about 60-70% of the drug (Rademaker-Lakhai et al., 2004; Leijen, 2013). From the results of Figure 2, one should expect that the use of ratios between NAMI-A and HSA in favor of the protein (for example those expected at the doses from 2.4 to 78.8 mg/m$^2$, corresponding respectively to ratios NAMI-A:HSA from 0.03 to 0.89) would favor the formation of the adduct in a relatively short time, leading to PK parameters different than those observed at doses of NAMI-A (for example 300-600 mg/m$^2$) leading to drug concentrations at the site

of injection higher than that of serum albumin. On the contrary, the perfectly linear PK found between 2.4 and 600 mg/m$^2$ suggests a behavior of the drug in vivo different than that expected from the present study of NAMI-A interactions with HSA performed in vitro. Indeed, one realistic hypothesis is that the drug, once in the blood, undergoes a number of chemical modifications and all the resulting compounds can easily react with the plasma proteins as illustrated in Scheme 1.

*Effects of reduction of the metal center.*

In the presence of ascorbic acid in ratios NAMI-A:ascorbic acid of 1:1, 2:1 and 40:1 the ruthenium drug is quite rapidly reduced (see Scheme 2). Reduction of NAMI-A should prevent the formation of inactive, probably toxic, aggregates in favor of the "active" species (Sava et al., 1999; Sava et al., 2002; Brindell et al., 2007). Correspondingly, when NAMI-A was reduced before injection into tumor bearing animals, the drug increased the activity against metastases and significantly reduced its toxicity to the host (Sava et al., 2002). Data reported in Figure 3, show that the reduction of $Ru^{+3}$ to $Ru^{+2}$ facilitates the formation of adducts with HSA as a function of the ratio NAMI-A:Ascorbic acid. Interestingly, also when only "traces" of the reducing agent are used (ratio NAMI-A:Ascorbic acid 1:0.025, the binding to albumin and the rate of chloride hydrolysis are markedly modified (Figure 3, middle panel). Considering that the human blood may contain 0.1-3.5x10$^{-5}$ M ascorbic acid but also other reducing agents such as glutathione (0.7-2x10$^{-3}$ M), we should expect that the drug finds a "reducing environment" quite suitable to induce its rapid reduction upon getting into the blood stream, and consequently favoring its binding to serum albumin (even traces of these reducing agents should switch on the process of reduction that subsequently goes by itself with an auto-catalytic progression (see Scheme 2).

The pharmacokinetic data reported in Table 1, obtained from mice treated by i.v. bolus of 50 mg/kg NAMI-A, or of the same drug previously reduced with an equimolar concentration of ascorbic acid, show, in this latter case, a significant reduction of the rate of the $\alpha$ phase of elimination with a corresponding increase of the AUC in the blood. In addition, the AUC value of the reduced drug in the lungs is significantly higher than that of

the unmodified drug, while no significant modification between the two forms of NAMI-A is found in the kidneys (Figure 4). The accumulation of the drug in the lungs shows a double step: an initial decay in the first 45 min following the end of infusion, independently of drug reduction before injection, followed by a progressive and significant increase of the lung concentration of the reduced drug, peaking at 4 h after drug injection (Figure 4, lower panel). The elimination by the kidneys does not show differences between reduced and non-reduced NAMI-A (Figure 4, upper panel) and that from the liver is similar to that from the lungs with a significant lower peak of ruthenium concentration per mg of tissue (about 5 ng/mg vs about 13 ng/mg) (Figure 4, middle panel).

*Effects of reduction and of HSA binding of NAMI-A on tumor cell adhesion.*

The evaluation of the effects of the formation of HSA-NAMI-A adducts combined with the reduction of the metal center on its pharmacological properties was tested on the capacity of the ruthenium drug to inhibit the adhesion properties of MDA-MB-231 cells in vitro. This test is a *bona fide* simulation of the capacity of NAMI-A to prevent the arrest of metastatic cells in a target organ/tissue. It can also be taken as an example of how the treated cells can detach from their substrate of growth and re-adhere on it during the mitotic events. HSA did not affect the adhesion of MDA-MB-231 cells to their plastic substrate of growth and, as expected, NAMI-A significantly reduced the re-adhesion of the treated cells to less than 20% of the untreated controls (Figure 5). The evaluation of the effects of the adducts NAMI-A-HSA on the re-adhesion capacity of the treated cells showed a significantly lower reduction than that of the free drug, independently of the ratio NAMI-A:HSA tested (Figure 5). Anyhow, the adducts with HSA caused a statistically significant reduction of the re-adhesion of the treated cells to about 30-40% of the untreated controls. Under conditions of cellular stress, as in growing tumor tissue, albumin is proposed to be taken up by cells as a source of amino acids and energy (Stehle et al., 1997). Thus, it is possible to argue that the adducts NAMI-A:HSA constitute a drug delivery system to tumor cells, and that NAMI-A could then perform its well known pharmacological activities, in particular in metastatic cells. Considering that the formation of adducts with serum albumin is responsible for a prolonged maintenance of the drug in the blood stream and of a

significantly higher AUC in the lungs, it could be speculated that, even if the overall potency is slightly reduced, the adduct NAMI-A:HSA might allow the drug to prolong its effects on the lung metastasis target. Further, it must be stressed that the lack of dependence of the biological effect studied on the ratio between NAMI-A and HSA suggests that the introduction of the drug into the blood stream (whatever daily dose is used at a conventional rate of infusion) should be irrelevant for the pharmacological effect.

The reduction of NAMI-A, at a 2:1 ratio with ascorbic acid, is responsible for a general mild increase of the anti re-adhesive properties of the antimetastatic drug on MDA-MB-231 cells at the higher doses tested (Figure 6). These data are consistent with the in vivo effects of NAMI-A, reduced in the tube immediately before injection and given to mice bearing MCa mammary carcinoma. They show a significantly greater effect of the drug on lung metastases as compared to controls treated with the parent drug alone (Sava et al., 2002). However, the reduction of NAMI-A with ascorbic acid in the presence of a 4-fold excess HSA, caused the inhibition of cell re-adhesion to about 40% of the untreated controls (Figure 7), an effect comparable to that caused by the adduct NAMI-A-HSA in the absence of any reduction (compare Figure 5 with Figure 7).

Overall, these data support the binding of NAMI-A to serum albumin, a reaction facilitated when the drug is in its reduced form and, in agreement with already reported data, the maintenance of the biological activity of the adduct formed with albumin (Brindell et al., 2008; Liu et al., 2010). The formation of the adduct is favored by low ratios NAMI-A:HSA and by the reduction of the drug. However, when injected in animals (and even more in humans), NAMI-A may bind also to the blood cells besides to plasma proteins. NAMI-A binding to cells was studied in vitro in many cell types showing a plateau within few minutes after cell challenge, indicative of specific binding on molecular determinant in the cell membrane (Frausin et al., 2002; Bacac et al., 2004; Frausin et al., 2005). However, unlike KP1019, NAMI-A does not get into the cell cytoplasm (Groessl et al., 2011; Aitken et al., 2012) and this observation may explain the rapid equilibrium established between bound and free NAMI-A when the milieu in which cells are kept in vitro is replaced with a new milieu free of the drug (Frausin et al., 2005). Given that red blood cells are a

significant constituent of the blood, it is therefore expected that a great amount of the injected drug is retained in the circulation and is slowly released simply to replace the free drug eliminated by kidneys by glomerular filtration. The slow release of the drug from the blood cells may also explain the relatively high $t_{1/2}$ of elimination. The different in vivo PK and the faster binding to albumin of the reduced NAMI-A seem to exclude that, even at low doses, the drug is rapidly reduced immediately upon injection. It can be then speculated that cell and protein binding prevails over reduction after in vivo administration. This observation supports the thesis that the reduction of the drug before injection must be considered relevant for the pharmacological activity, supporting the relevance of the corresponding patent (Mestroni et al., 2001).

**Acknowledgements.** The permission to perform the chemical studies at the Department of Chemical and Pharmaceutical Sciences of the University of Trieste is gratefully appreciated. The chemical and biological contribution by N.V. and Z.J. at Callerio Foundation Onlus in Trieste was supported by the student project of the Palacky University in Olomouc (Grant PrF 2014 029) and by Operational Program Education for Competitiveness – European Social Fund (CZ 1.07/2.3.00/20.0057). Work entirely funded by Callerio Foundation Onlus.

**References**

Aitken JB, Antony S, Weekley CM, Lai B, Spiccia L, Harris HH. Distinct cellular fates for KP1019 and NAMI-A determined by X-ray fluorescence imaging of single cells. Metallomics, 2012, 4: 1051-6.

Alessio E, Mestroni G, Bergamo A, Sava G. Ruthenium antimetastatic agents. Curr Top Med Chem, 2004, 4: 1525-35.

Antonarakis ES, Emadi A. Ruthenium-based chemotherapeutics: are they ready for prime time? Cancer Chemother Pharmacol, 2010, 66: 1-9.

Ascone I, Messori L, Casini A, Gabbiani C, Balerna A, Dell'Unto F, Congiu Castellano A. Exploiting soft and hard X-ray absorption spectroscopy to characterize metallodrug/protein interactions: the binding of [*trans*-$RuCl_4$(Im)(dimethyl-sulfoxide)][Im] (Im = imidazole) to bovine serum albumin. Inorg Chem, 2008, 47: 8629-34.

Bacac M, Hotze ACG, van der Schilden K, Haasnoot JG, Pacor S, Alessio E, Sava G, Reedijl J. The hydrolysis of the anti-cancer ruthenium complex NAMI-A affects its DNA binding and antimetastatic activity: an NMR evaluation. J Inorg Biochem, 2004, 98: 402-12.

Bergamo A, Delfino R, Casarsa C, Sava G. CDK1 hyperphosphorylation maintenance drives the time-course of G2-M cell cycle arrest after short treatment with NAMI-A in KB cells. Anti-Cancer Agents in Med Chem, 2012, 12: 949-58.

Bergamo A, Gagliardi R, Scarcia V, Furlani A, Alessio E, Mestroni G, Sava G. In vitro cell cycle arrest, in vivo action on solid metastasizing tumors, and host toxicity of the antimetastatic drug NAMI-A and cisplatin. JPET, 1999, 289: 559-64.

Bergamo A, Messori L, Piccioli F, Cocchietto M, Sava G. Biological role of adduct formation of the ruthenium(III) complex NAMI-A with serum albumin and serum transferrin. Invest New Drugs, 2003, 21: 401-11.

Bouma M, Nuijen B, Jansen MT, Sava G, Flaibani A, Bult A, Beijnen JH. A kinetic study of the chemical stability of the antimetastatic ruthenium complex NAMI-A. Int J Pharmaceutics, 2002, 248: 239-46.

Brindell M, Piotrowska D, Shoukry AA, Stochel G, van Eldik R. Kinetics and mechanism of the reduction of (ImH) [*trans*-$RuCl_4$(dmso)(Im)] by ascorbic acid in acidic solution. J Biol Inorg Chem, 2007, 12: 809-18.

Brindell M, Stawoska I, Supel J, Skoczowski A, Stochel G, van Eldik R. The reduction of (Im)]*trans*-$Ru^{III}Cl_4$(dmso)(Im)] under physiological conditions: preferential reaction of the reduced complex with human serum albumin. J Biol Inorg Chem, 2008, 13: 909-18.

Deng JY, Liang H. Clinical significance of lymph node metastasis in gastric cancer. World J Gastroenterol, 2014, 20: 3967-75.

Frausin F, Cocchietto M, Bergamo A, Scarcia V, Furlani A, Sava G. Tumour cell uptake of the metastasis inhibitor ruthenium complex NAMI-A and its in vitro effects on KB cells. Cancer Chemother Pharmacol, 2002, 50: 405-11.

Frausin F, Scarcia V, Cocchietto M, Furlani A, Serli B, Alessio E, Sava G. Free exchange across cells, and echistatin-sensitive membrane target for the metastasis inhibitor NAMI-A (Imidazolium *trans*-Imidazole dimethyl sulfoxide tetrachlororuthenate) on KB tumor cells. J Pharmacol Exp Ther, 2005, 313: 227-33.

Gava B, Zorzet S, Spessotto P, Cocchietto M, Sava G. Inhibition of B16 melanoma metastases with the ruthenium complex imidazolium trans-imidazoledimethyl-sulfoxidetetrachlororuthenate and down-regulation of tumor cell invasion. JPET, 2006, 317: 284-91.

Groessl M, Zava O, Dyson PJ. Cellular uptake and subcellular distribution of ruthenium-based metallodrugs under clinical investigation versus cisplatin. Metallomics, 2011, 3: 591-9.

Hartinger CG, Jakupec MA, Zorbas-Seifried S, Groessl M, Egger A, Berger W, Zorbas H, Dyson PJ, Keppler BK. KP1019, a new redox-active anticancer agent – Preclinical development and results of a clinical phase I study in tumor patients. Chem & Biodiversity, 2008, 5: 2140-55.

Hartinger CG, Zorbas-Seifried S, Jakupec MA, Kynast B, Zorbas H, Keppler BK. From bench to bed side – preclinical and early clinical development of the anticancer agent indazolium *trans*-[tetrachlorobis(1*H*-indazole)ruthenate(III)] (KP1019 or FFC14A. J Inorg Biochem, 2006, 100: 891-904.

Hostetter AA, Osborn MF, DeRose VJ. RNA-Pt adducts following cisplatin treatment of Saccharomyces cerevisiae. ACS Chem Biol, 2012, 7: 218-25.

Komeda S and Casini A. Next-generation anticancer metallodrugs. Curr Top Med Chem, 2002, 12: 219-35.

Leijen S. Development of combination therapy with anti-cancer drugs. PhD Thesis University of Utrecht.

Levina A, Aitken JB, Gwee YY, Lim ZJ, Liu M, Singharay AM, Wong PF, Lay PA. Biotransformation of anticancer Ruthenium(III) complexes: an X-ray absorption spectroscopic study. Chem Eur J, 2013, 19: 3609-19.

Liu M, Lim ZJ, Gwee YY, Levina A, Lay PA. Characterization of a Ruthenium(III)/NAMI-A adduct with bovine serum albumin that exhibits a high anti-metastatic activity. Angew Chem Int Ed, 2010, 49: 1661-4.

McCusker M, Basset-Seguin N, Dummer R, Lewis K, Schadendorf D, Sekulic A, Hou J, Wang L, Yue H, Hauschild A. Metastatic basal cell carcinoma: prognosis dependent on anatomic site and spread of disease. Eur J Cancer, 2014, 50: 774-83.

McLoughlin JM, Jensen EH, Malafa M. Resection of colorectal liver metastases: current perspectives. Cancer Control, 2006, 13: 32-41.

Meng X, Leyva ML, Jenny M, Gross I, Benosman S, Fricker B, Harlepp S, Hebraud P, Boos A, Wlosik P, Bischoff P, Sirlin C, Pfeffer M, Loeffler JP, Gaiddon C. A ruthenium-containing organometallic compound reduces tumor growth through induction of the endoplasmic reticulum stress gene CHOP. Cancer Res, 2009, 69: 5458-66.

Messori L, Orioli P, Vullo D, Alessio E, Iengo E. A spectroscopic study of the reaction of NAMI, a novel ruthenium(III) anti-neoplastic complex, with bovine serum albumin. Eur J Biochem, 2000, 267: 1206-13.

Mestroni G, Alessio E, Sava G. New salts of anionic complexes of Ru(III) as antimetastatic and antineoplastic agents. International Patent PCT C 07F 15/00 A61K 31/28, WO 98/00431, 1998.

Mestroni G, Alessio E, Sava G, Iengo E, Zorzet S, Bergamo A. Ruthenium(II) complexes with high antitumoral and antimetastatic activities. International Patent ITMI992256/A1, WO0130789 (A1), 2001.

Page SM, Boss SR, Barker PD. Tuning heavy metal compounds for anti-tumor activity: is diversity the key to ruthenium's success? Future Med Chem, 2009, 1: 541-559.

Rademaker-Lakhai JM, van den Bongard D, Pluim D, Beijnen JH, Schellens JHM. A phase I and pharmacological study with imidazolium-*trans*-DMSO-imidazole-tetrachlororuthenate, a novel ruthenium anticancer agent. Clin Cancer Res, 2004, 10: 3717-27.

Sava G, Alessio E, Bergamo A, Mestroni G. Sulfoxide ruthenium complexes: non-toxic tools for the selective treatment of solid tumour metastases. In: Topics in Biological Inorganic Chemistry, Clarke MJ, Sadler PJ (eds), Springer, Berlin, 1999, pp 143-69.

Sava G, Bergamo A, Zorzet S, Gava B, Casarsa C, Cocchietto M, Furlani A, Scarcia V, Serli B, Iengo E, Alessio E, Mestroni G. Influence of chemical stability on the activity of the antimetastasis ruthenium compound NAMI-A. Eur J Cancer, 2002, 38: 427-35.

Sava G, Capozzi I, Clerici K, Gagliardi R, Alessio E, Mestroni G. Pharmacological control of lung metastases of solid tumours by a novel ruthenium complex. Clin Exp Metastasis, 1998, 16: 371-9.

Sava G, Clerici K, Capozzi I, Cocchietto M, Gagliardi R, Alessio E, Mestroni G, Perbellini A. Reduction of lung metastasis by ImH[trans-RuCl4(DMSO)Im]: mechanism of the selective action investigated on mouse tumors. Anti-Cancer Drugs, 1999, 10: 129-38.

Skehan P, Soreng R, Scudiero D, Monks A, McMahon J, Vistica D, Warren JT, Bokesch H, Kenney S, Boyd MR. New colorimetric cytotoxicity assay for anticancer-drug screening. J Natl Cancer Inst, 1990, 82: 1107-12.

Stehle G, Sinn H, Wunder A, Schrenk HH, Stewart JCM, Hartung G, Maier-Borst W, Heene DL. Plasma protein (albumin) catabolism by the tumor itself – implications for tumor metabolism and the genesis of cachexia. Crit Rev Oncol/Hematol, 1997, 26: 77-100.

Webb MI, Walsby CJ. Control of ligand-exchange processes and the oxidation state of the antimetastatic Ru(III) complex NAMI-A by interactions with human serum albumin. Dalton Trans, 2011, 40: 1322-31.

## Legend to Figures

**Figure 1.** Spectrophotometric pattern of the chemical transformation of NAMI-A. 400 μM NAMI-A were monitored up to 145 min. Medium: Dulbecco's phosphate buffered saline (DPBS) pH 7.4, temperature: 25 °C, spectra range: from 700 to 300 nm, scanning speed: 200 nm/min, band: 1.0 nm, data pitch: 1.0 nm, interval of measurements: 5 min, volume: 3 ml.

**Figure 2.** Effects of human serum albumin (HSA) on the chemical transformation of NAMI-A.

100 μM NAMI-A were exposed to different concentrations of HSA and the reaction was monitored up to 145 min. NAMI-A:HAS ratios at 4:1 (upper panel, left), 2:1 (upper panel, right), 1:1 (lower panel, left) and 0.25:1 (lower panel, right). Medium: DPBS pH 7.4, temperature: 25 °C, spectra range: from 700 to 300 nm, scanning speed: 200 nm/min, band: 1.0 nm, data pitch: 1.0 nm, interval of measurements: 5 min, volume: 3 ml.

**Figure 3.** Effects of ascorbic acid on the chemical transformation of NAMI-A in the presence of HSA.

400 μM (upper and middle panels) or 200 μM (lower panel) NAMI-A were reduced with ascorbic acid in the presence of HSA. Final ratios NAMI-A:HAS:ascorbic acid were respectively 4:1:1 (upper panel), 4:1:0.025 (middle panel), 2:1:1 (lower panel). Medium: DPBS pH 7.4, temperature: 25 °C, spectra range: from 700 to 300 nm, scanning speed: 200 nm/min, band: 1.0 nm, data pitch: 1.0 nm, interval of measurements: 5 min, volume: 3 ml. Theoretical time zero was calculated as the sum of the spectra for all the reaction components measured in separate solutions. This experimental approach was used to mimic the situation at the beginning of the reaction without the use of stopped-flow technique.

**Figure 4.** Ruthenium concentration profiles after intravenous injection of NAMI-A in CD1 male mice.

50 mg/kg NAMI-A was dissolved, immediately before use, in an appropriate volume of DPBS or of DPBS containing an equivalent amount of ascorbic acid (NAMI-A:ascorbic acid ratio 1:1) for 10 min, in order to inject 0.05 ml/10 g body weight (NAMI-A $Ru^{+3}$, continuous line; NAMI-A $Ru^{+2}$, dotted line). Ruthenium concentration in the kidney, liver and lung are reported in the upper, central and lower panel, respectively. The AUC values for kidney, liver and lung are expressed as mg $Ru{*}L^{-1}{*}h$. Ruthenium was quantified by AAS.

**Figure 5.** Effect of NAMI-A and of NAMI-A-HSA adducts treatments on the re-adhesion of MDA-MB-231 cells.

Cells were sown in complete medium and allowed to grow for 2 days at 37 °C, 5% $CO_2$ before the complete medium was replaced with serum-starved medium containing 0.1% w/v BSA for 24 h. Treatment with 100 μM NAMI-A was performed for 1 h at 37 °C in the presence of HSA at ratios NAMI-A:HSA of 1:0.25, 1:0.5, 1:1, 1:4. At the end of the treatment cells were detached and left to re-adhere on a new culture well for 30 min; adhered cells were detected by the SRB test. Data represent the mean±S.D. values of three separate experiments, each performed in quadruplicate. Statistical analysis: One-Way Analysis of Variance (ANOVA) and Tukey-Kramer Multiple Comparisons Test. (a) $p<0.001$ and (b) $p<0.01$ vs. untreated controls; (c) $p<0.01$ and (d) $p<0.001$ vs. NAMI-A; (e) $p<0.001$ vs. the same dose of HSA without NAMI-A.

**Figure 6.** Effect of reduced NAMI-A on the re-adhesion of MDA-MB-231 cells.

Cells were sown in complete medium and allowed to grow for 2 days at 37 °C, 5% $CO_2$ before the complete medium was replaced with serum-starved medium containing 0.1% w/v BSA for 24 h. Treatment with 1, 10, 20 and 100 μM NAMI-A was performed for 1 h at 37 °C in the presence of ascorbic acid at ratios NAMI-A:ascorbic acid of 1:0.5 and 2:1. At the end of the treatment cells were detached and left to re-adhere on a new culture well for 30 min; adhered cells were detected by the SRB test. Data represent the mean±S.D. values of three separate experiments, each performed in quadruplicate. Statistical analysis: One-Way Analysis of Variance (ANOVA) and Tukey-Kramer Multiple Comparisons Test. (a) $p<0.001$ vs. untreated controls.

**Figure 7.** Effect of reduced NAMI-A-HSA adducts on the re-adhesion of MDA-MB-231 cells.

Cells were sown in complete medium and allowed to grow for 2 days at 37 °C, 5% $CO_2$ before the complete medium was replaced with serum-starved medium containing 0.1% w/v BSA for 24 h. Treatment with 100 μM NAMI-A was performed for 1 h at 37 °C in the presence of 100 μM ascorbic acid and 400 μM HSA (ratio NAMI-A:HAS:ascorbic acid of 1:4:1. At the end of the treatment cells were detached and left to re-adhere on a new culture well for 30 min; adhered cells were detected by the SRB test. Data represent the mean±S.D. values of three separate experiments, each performed in quadruplicate. Statistical analysis: One-Way Analysis of Variance (ANOVA) and Tukey-Kramer Multiple Comparisons Test. (a) $p<0.001$ vs. untreated controls; (b) $p<0.001$ vs. NAMI-A+ascorbic acid+HSA.

**Scheme 1.** Probable chemical modifications occurring on NAMI-A after intravenous bolus injection and binding to serum proteins. Modified from: Webb and Walsby, 2001; Liu et al., 2010; Levina et al., 2013.

**Scheme 2.** Chemical modifications of NAMI-A in solution at pH 7.4 at 25 °C leading to the formation of the reactive species.

Table 1. Pharmacokinetic data for bi-compartment distribution of NAMI-A in CD1 mouse

| Compound | $t_{1/2}$ (h) | | Vd | $Cl_{tot}$ | $AUC_{0\rightarrow\infty}$ |
|---|---|---|---|---|---|
| | α | β | (mL) | (mL·h$^{-1}$) | (mg Ru·L$^{-1}$·h) |
| NAMI-A($Ru^{+3}$) | 0.07 | 14.4 | 23.3 | 1.21 | 354 |
| NAMI-A($Ru^{+2}$) | 0.32 | 12.8 | 14.1 | 0.71 | 668 |

Data were obtained by analysis of ruthenium plasma concentration applying a bi-compartment model (β phase starting from 0,666 h). NAMI-A was reduced 1:1 with ascorbic acid for 10 min before i.v. administration on CD1 mice. Ruthenium was quantified on samples, diluted by water, by AAS technique.

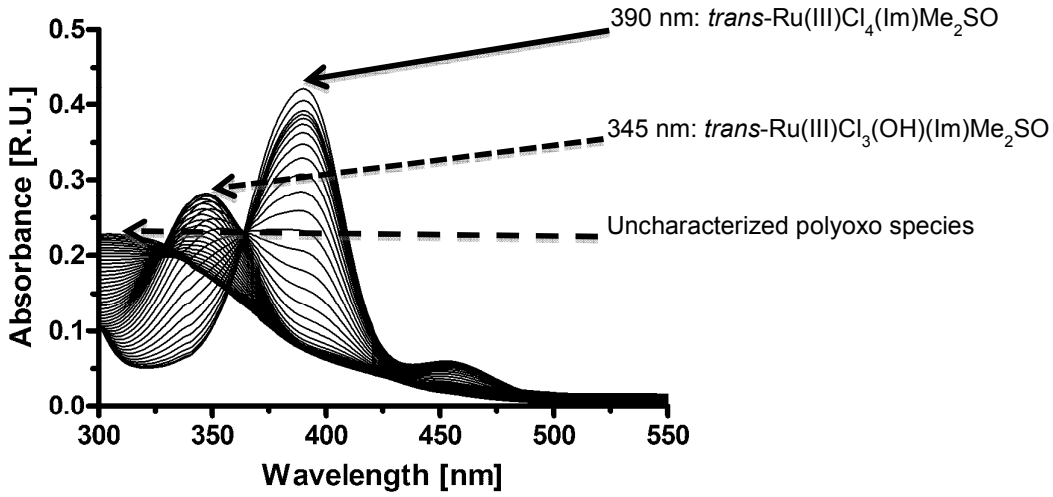


Figure 1. Spectrophotometric pattern of the chemical transformation of NAMI-A.

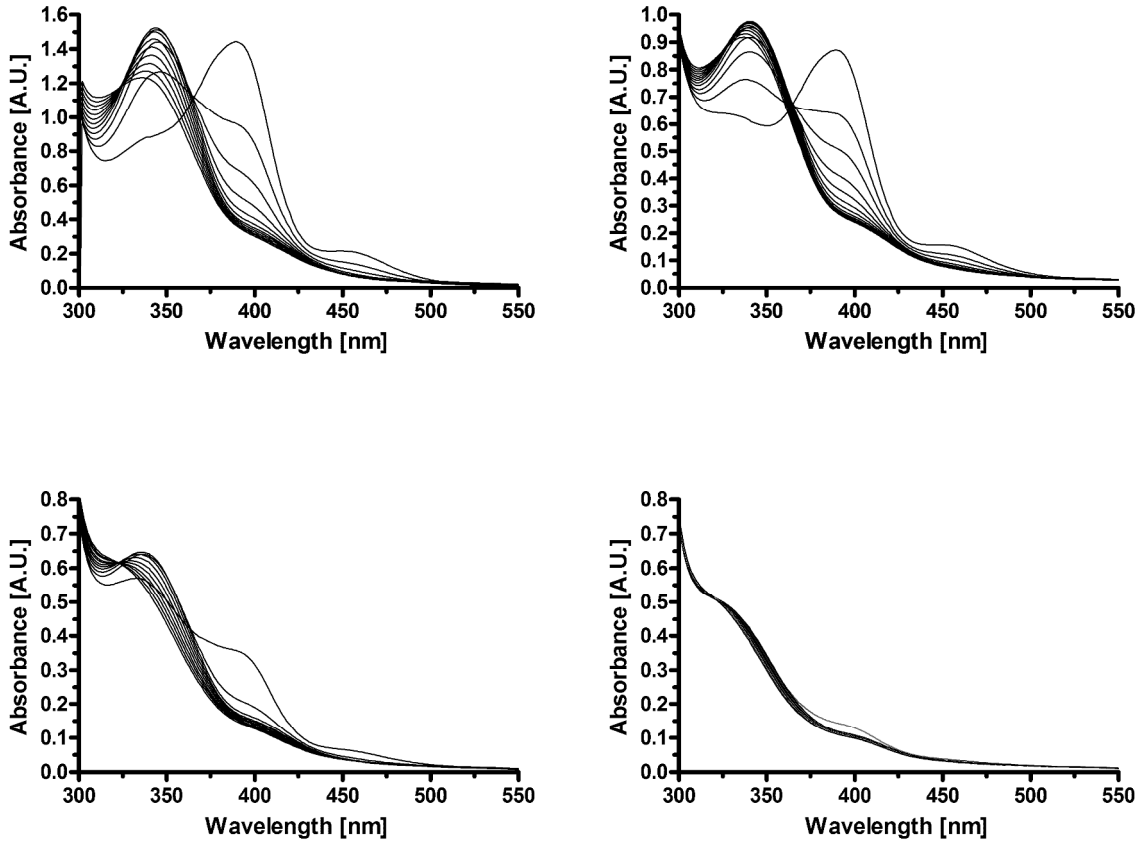


Figure 2. Effects of human serum albumin (HSA) on the chemical transformation of NAMI-A.

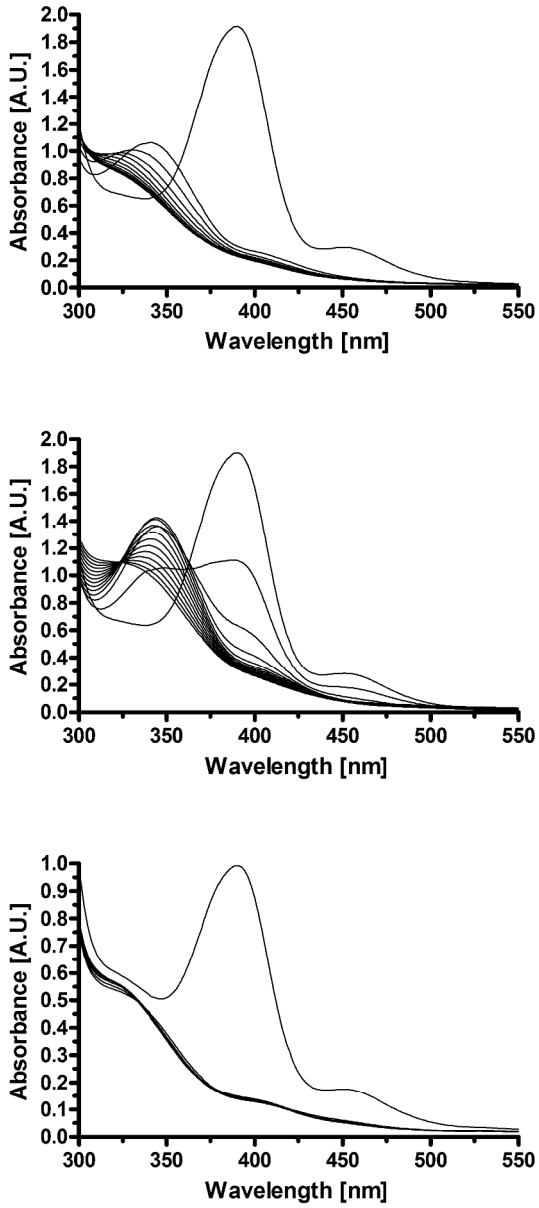


Figure 3. Effects of ascorbic acid on the chemical transformation of NAMI-A in the presence of HSA.

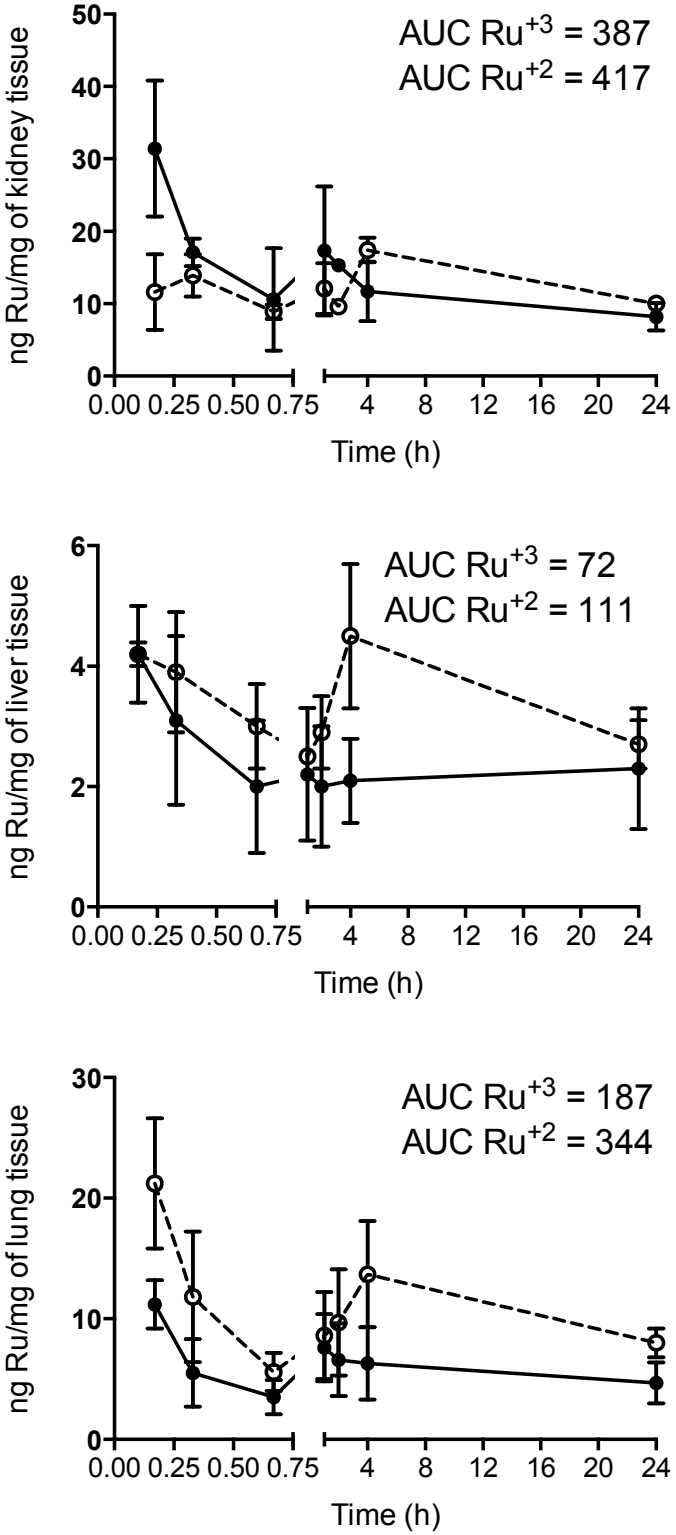


Figure 4. Ruthenium concentration profiles after intravenous injection of NAMI-A in CD1 male mice.

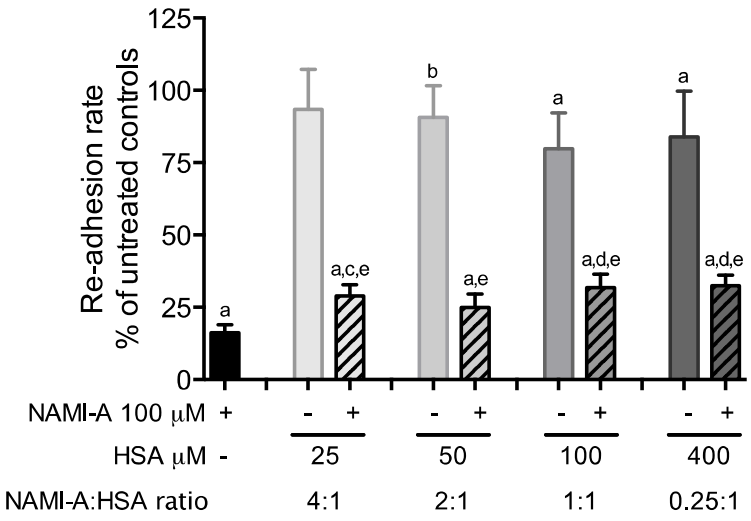


Figure 5. Effect of NAMI-A and of NAMI-A-HSA adducts treatments on the re-adhesion of MDA-MB-231 cells.

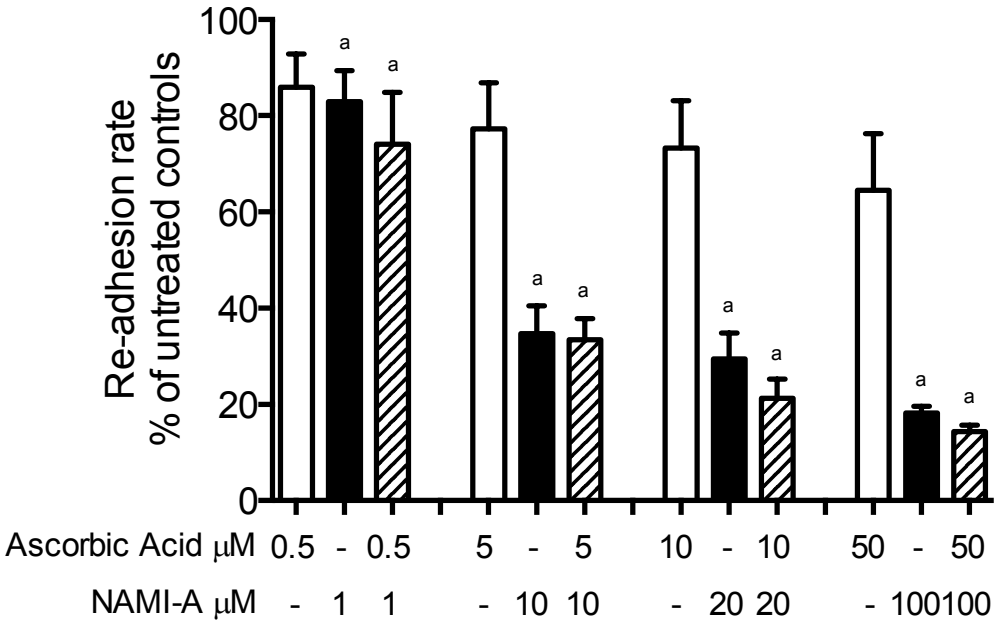


Figure 6. Effect of reduced NAMI-A on the re-adhesion of MDA-MB-231 cells.

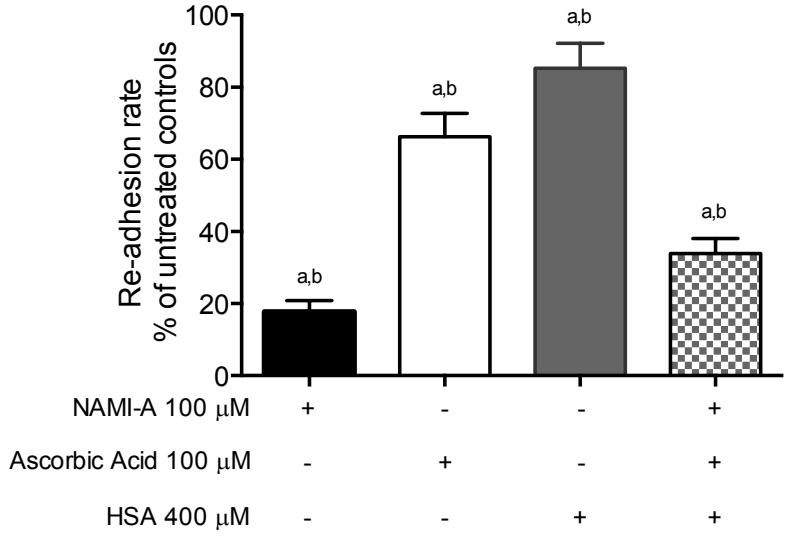


Figure 7. Effect of reduced NAMI-A-HSA adducts on the re-adhesion of MDA-MB-231 cells.

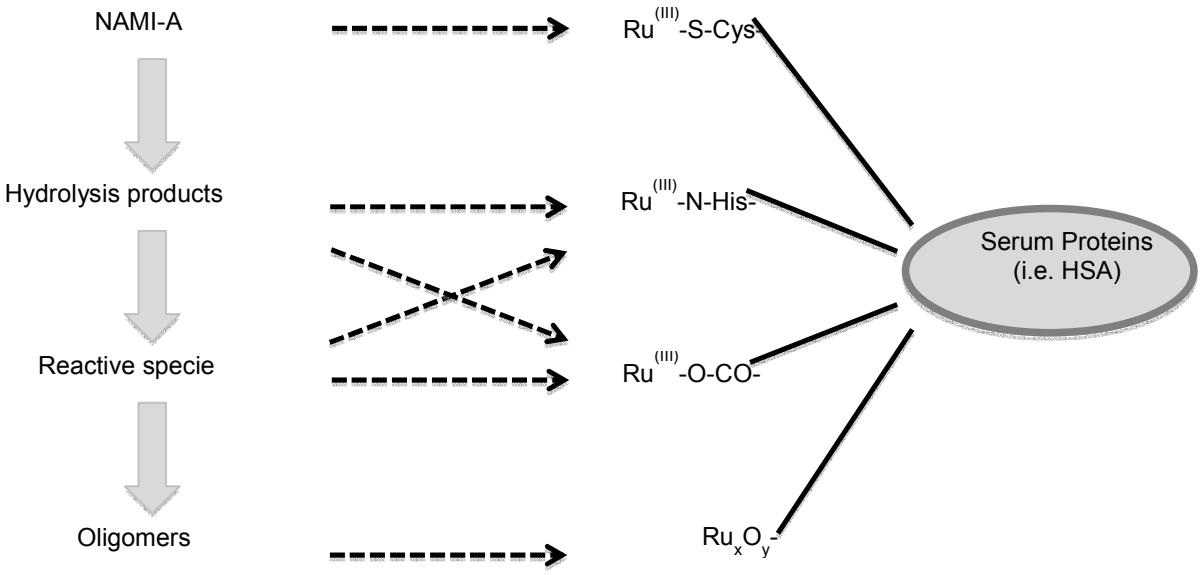


Modified from: Webb and Walsby, 2001; Liu et al., 2010; Levina et al., 2013

Scheme 1. Binding of expected NAMI-A "metabolites" to serum albumin.

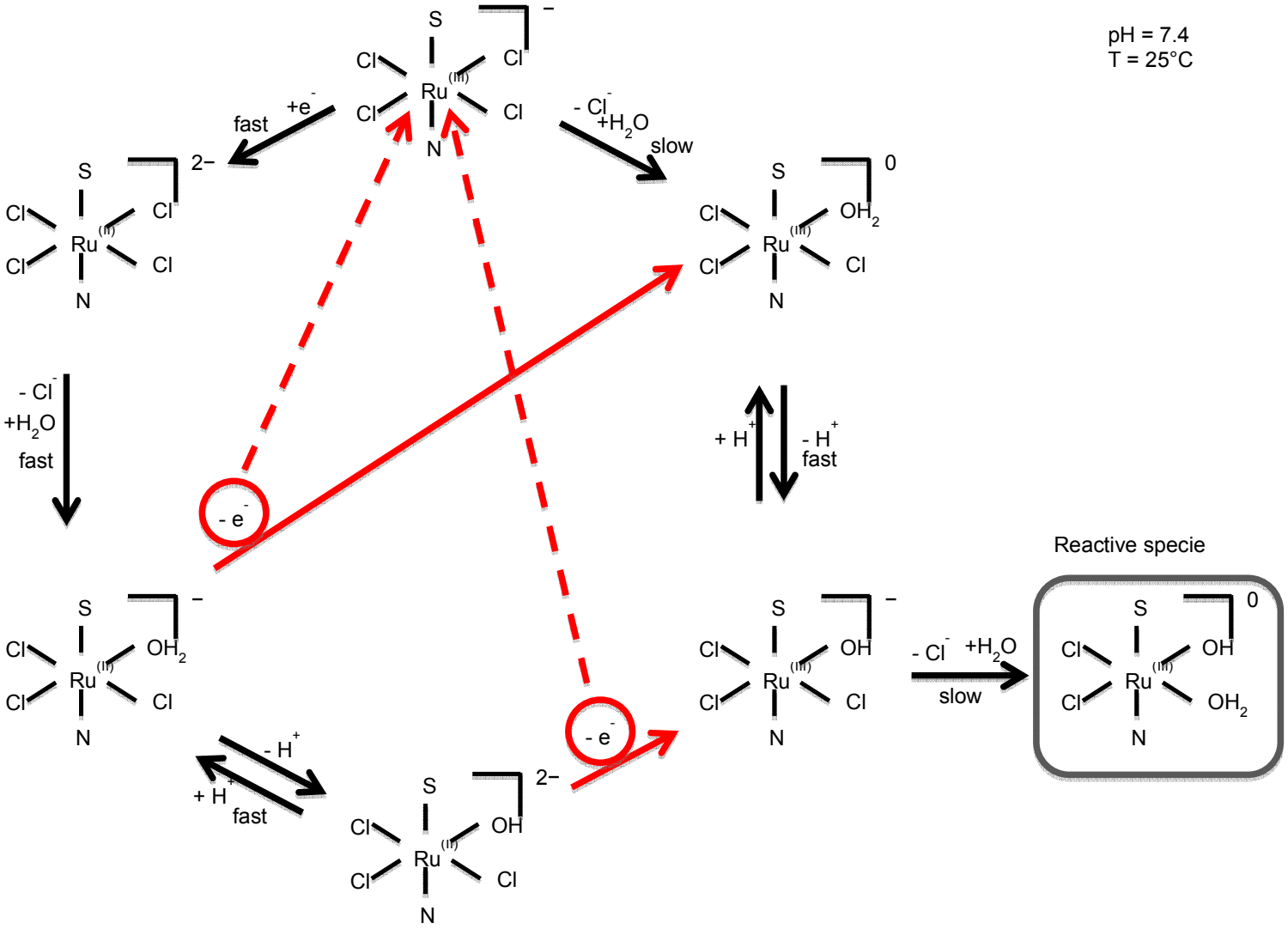


Scheme 2. Possible chemical transformations of NAMI-A in solution.

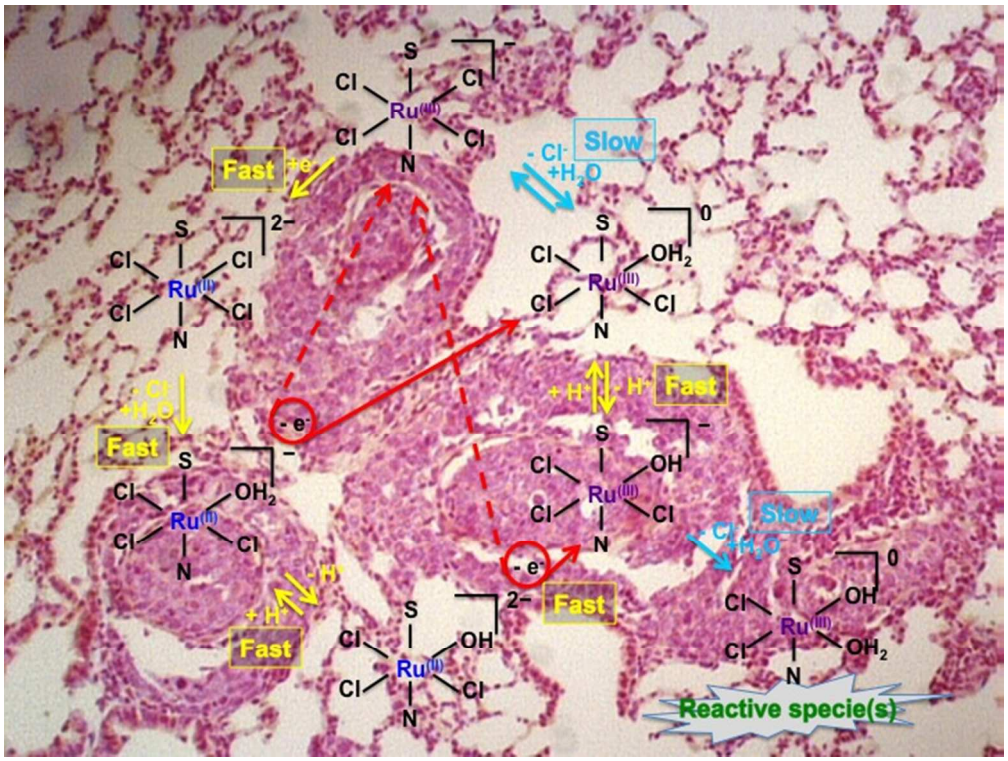


Chemical transformations of NAMI-A in biological environments
254x190mm (72 x 72 DPI)